SAND2012-6060C

Optimization-Based Remap and Transport: Part 2

A Divide and Conquer Strategy for Feature-Preserving Discretizations

Denis Ridzal, Pavel Bochev, and Kara Peterson
Sandia National Laboratories

Workshop on Modeling and Simulation of Transport Phenomena
The Moselle Valley, July 30 – August 1, 2012

Supported in part by U.S. DEPARTMENT OF ENERGY | Office of Science, ASCR, ASC

National Nuclear Security Administration

Sandia National Laboratories is a multi-program laboratory managed and operated by Sandia Corporation, a wholly owned subsidiary of Lockheed Martin Corporation, for the U.S. Department of Energy's National Nuclear Security Administration under contract DE-AC04-94AL85000

Sandia National Laboratories

Outline: Part 2

- Optimization algorithms
- Robustness and accuracy studies
- Efficiency studies
- Extension to optimization-based transport

Acknowledgments

G. Scovazzi
SNL

J. Young
SNL

M. Shashkov
LANL

Flux Variable-Flux Target OBR

OBR-FVFT = global inequality constrained QP

$$\underset{F_{ij}^h}{\text{minimize}} \quad \sum_{Cell} \sum_{Flux} \left(F_{ij}^h - F_{ij}^T\right)^2 \quad \text{subject to}$$

$$\tilde{m}_i^{min} \le m_i + \sum_{i<j} F_{ij}^h - \sum_{i>j} F_{ji}^h \le \tilde{m}_i^{max} \qquad i = 1,\ldots,N$$

⬅ **C1 & C2**

⬅ **C3**

Theorem. (Existence of unique optimal solutions)

The OBR-FVFT feasible set is non-empty: for any given density distribution there exists a set of antisymmetric fluxes which satisfy the global inequality constraints.

Connection with state-of-the-art FCR

Change of variables

$$F_{ij}^h = (1-\alpha_{ij})F_{ij}^L + \alpha_{ij}F_{ij}^T = F_{ij}^L + \alpha_{ij}dF_{ij}, \quad dF_{ij} = F_{ij}^T - F_{ij}^L, \quad \alpha_{ij} = \alpha_{ji}$$

After changing variables the OBR-FVFT QP transforms as follows

Objective

$$\left\| F_{ij}^h - F_{ij}^T \right\| = \left|(1-\alpha_{ij})\right| \left\| dF_{ij} \right\|$$

Constraint

$$\tilde{Q}_i^{\min} \le \sum_{i<j} \alpha_{ij} dF_{ij} - \sum_{i>j} \alpha_{ij} dF_{ij} \le \tilde{Q}_i^{\max} \quad i = 1,\ldots,N$$

where

$$\tilde{Q}_i^{\min} = \tilde{m}_i^{\min} - \tilde{m}_i^L \le 0 \quad \text{and} \quad \tilde{Q}_i^{\max} = \tilde{m}_i^{\max} - \tilde{m}_i^L \ge 0$$

*Liska et al, Optimization-based synchronized flux-corrected conservative interpolation (remapping) of mass and momentum for ALE methods, **Journal of Computational Physics**, 2010, pp.1467-1497*

Theorem.

FCR is a global constrained optimization problem such that

(1) The FCR objective function **is equivalent** to the OBR objective.

(2) The FCR feasible set is **always a subset** of the OBR feasible set.

OBR

$$\underset{F_{ij}^h}{\text{minimize}} \quad \sum_{Cell} \sum_{Flux} \left(1-\alpha_{ij}\right)^2 \left(dF_{ij}\right)^2 \quad \text{subject to}$$

$$\tilde{Q}_i^{\min} \le \sum_{i<j} \alpha_{ij} dF_{ij} - \sum_{i>j} \alpha_{ij} dF_{ij} \le \tilde{Q}_i^{\max} \qquad i = 1,\ldots,N$$

FCR

$$\underset{F_{ij}^h}{\text{minimize}} \quad \sum_{Cell} \sum_{Flux} \left(1-\alpha_{ij}\right)^2 \left(dF_{ij}\right)^2 \quad \text{subject to}$$

$$\begin{cases} D_i^- dF_{ij} \le \alpha_{ij} dF_{ij} \le 0 & \text{for} \quad i<j, \quad dF_{ij} \le 0 \\ D_i^- dF_{ij} \ge \alpha_{ij} dF_{ij} \ge 0 & \text{for} \quad i>j, \quad dF_{ij} \ge 0 \end{cases} \qquad \begin{cases} 0 \le \alpha_{ij} dF_{ij} \le D_i^+ dF_{ij} & \text{for} \quad i<j, \quad dF_{ij} \ge 0 \\ 0 \ge \alpha_{ij} dF_{ij} \ge D_i^+ dF_{ij} & \text{for} \quad i>j, \quad dF_{ij} \le 0 \end{cases}$$

FCR can be viewed as approximation of OBR obtained by replacing the OBR constraints set by a simpler set of box constraints

Impacts of the smaller FCR feasible set

The "torture" test

Designed to test
topology preservation

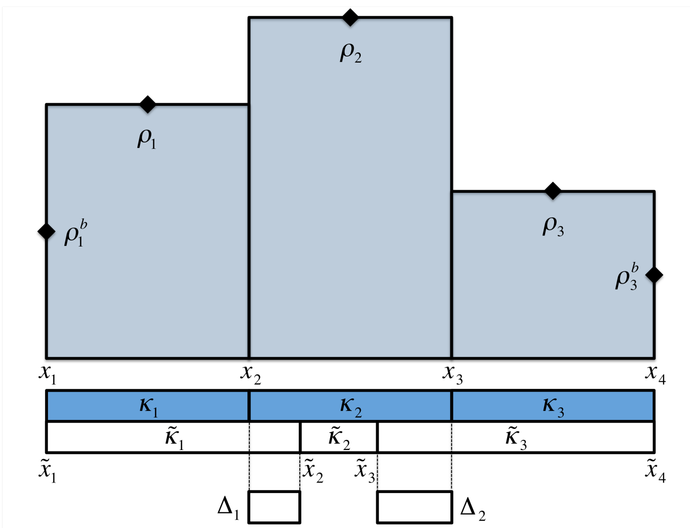

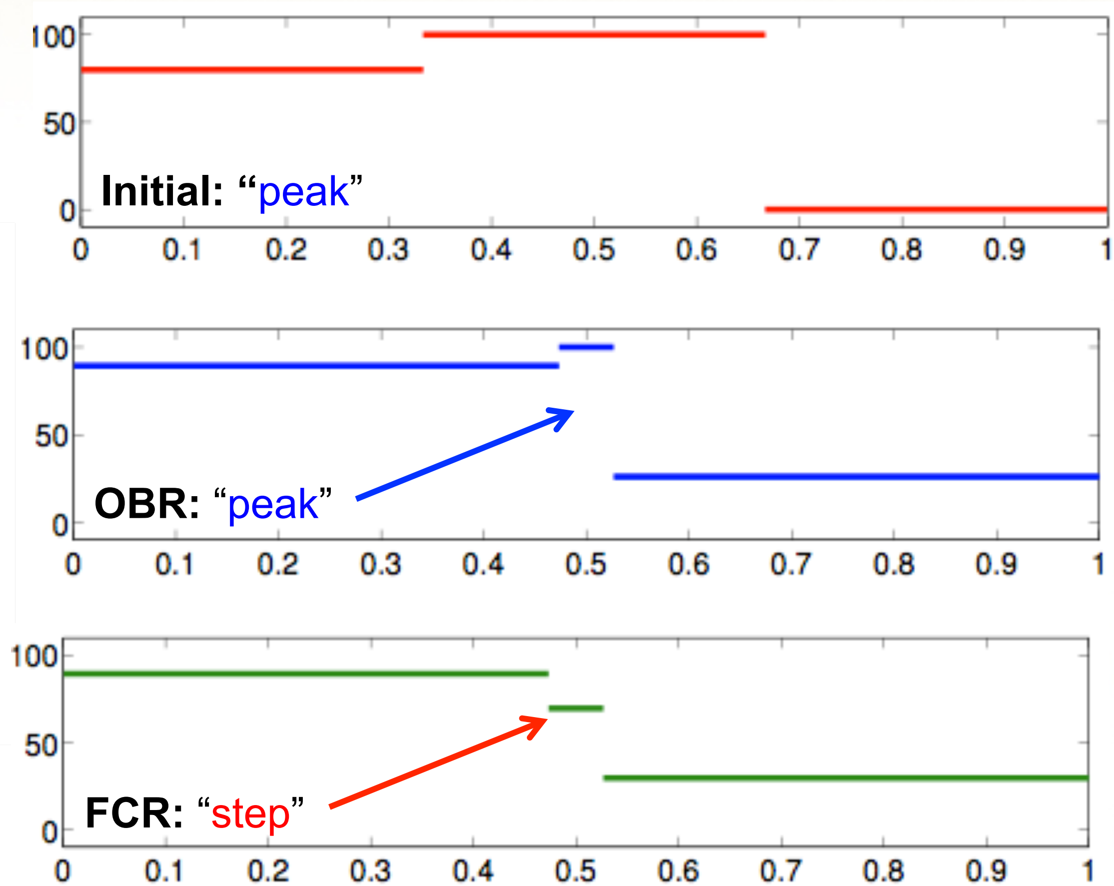

FCR does not preserve the shape of the peak density distribution
May be improved by using iterated FCR

Deconstructing the torture test

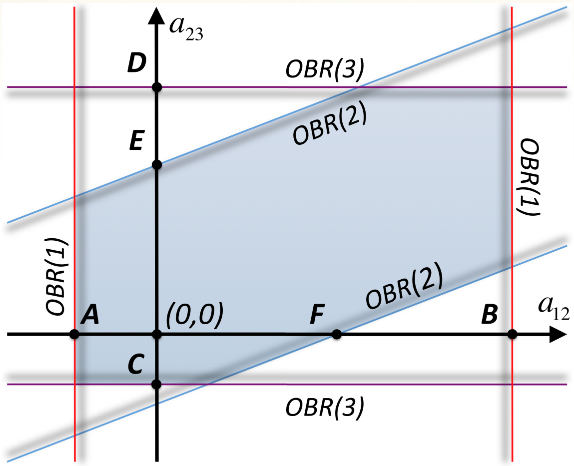

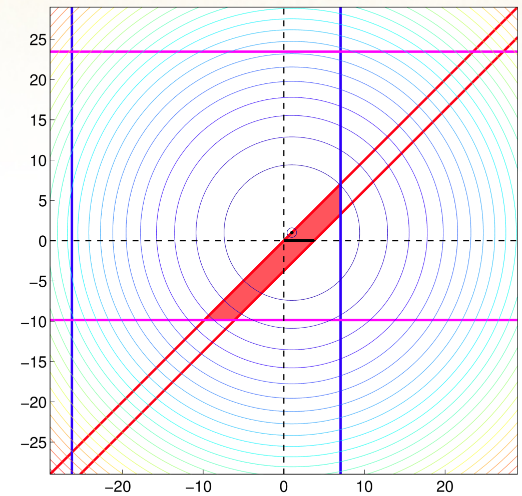

OBR feasible set

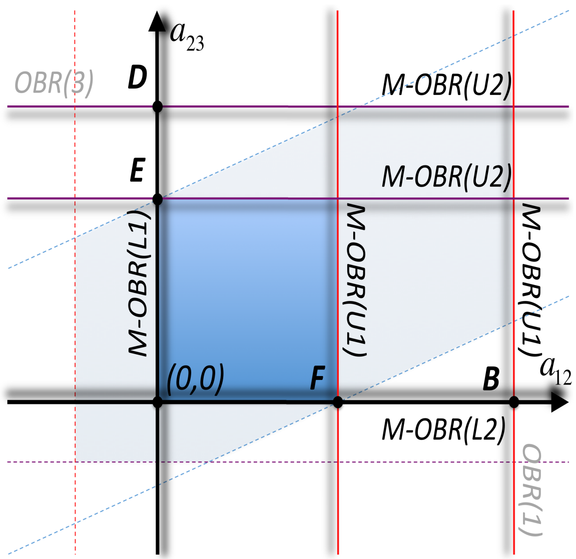

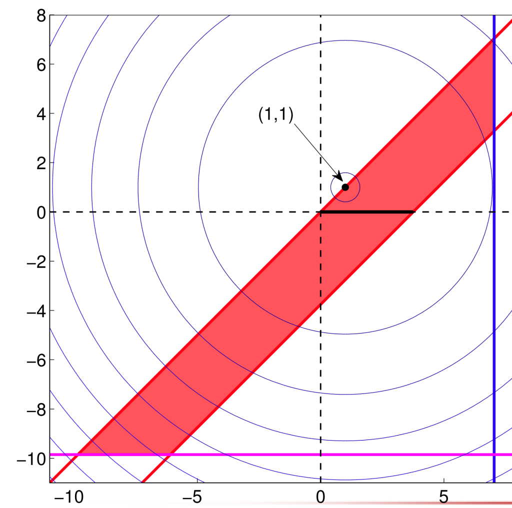

FCR feasible set

Swept region implementation

Exact cell intersections

Dukowicz, 1984

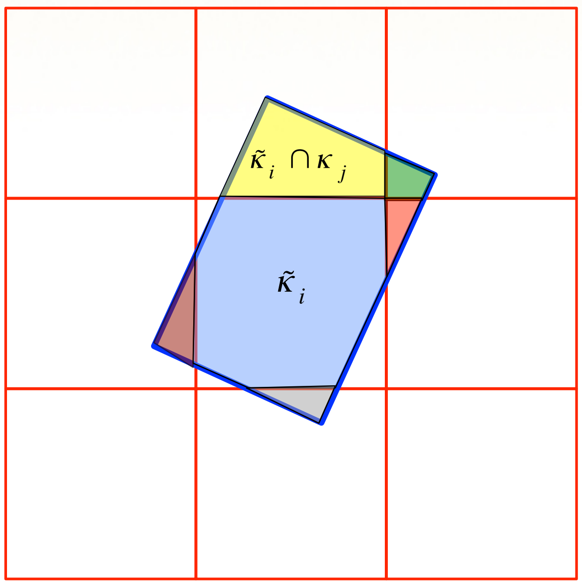

Swept region (SR) approximation

Margolin, Shashkov, 2003

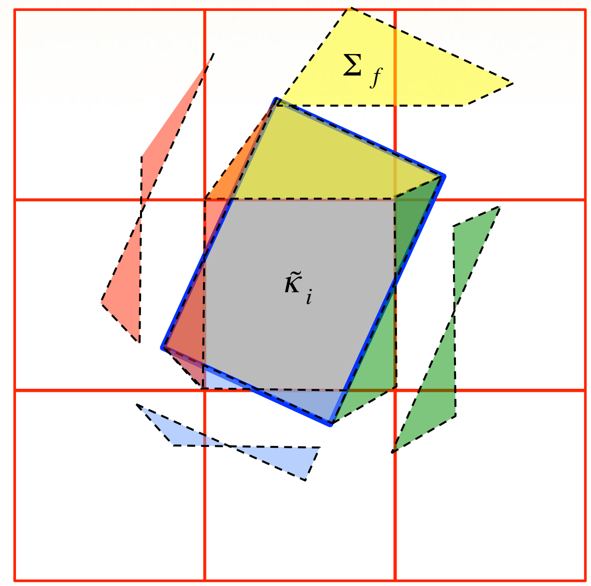

$$\tilde{m}_i^h = m_i^h + \sum_{E(\tilde{\kappa}_i)} F_{ij}^h$$

$$F_{ij}^h = \int_{\tilde{\kappa}_i \cap \kappa_j} \rho_i^h(x)dV - \int_{\kappa_i \cap \tilde{\kappa}_j} \rho_i^h(x)dV$$

$$F_{ij}^h = \int_{\Sigma_f} \rho_i^h(x)dV$$

SRs are completely determined by the coordinates of old and new cells ⇒ **efficiency**

SRs give exact cell masses for linear density ⇒ **accuracy**

Exact cell intersections guarantee that low order fluxes in FCR are monotone. However, this is not true for SR without additional restrictions on mesh motion.

Potential issue for FCR but not for OBR, which does not use low order fluxes

Sandia National Laboratories

OBR-FVFT Robustness (SR Implementation)

Preservation of monotonicity

	C=5	C=6	C=7	C=14	C=15	C=16	C=100
OBR	✔	✔	✔	✔	✔	✔	✔
FCR	✔	✔	✔	✗	✗	✗	✗
Donor	✔	✗	✗	✗	✗	✗	✗

Preservation of linearity

	C=3	C=4	C=5	C=15	C=16	C=100
OBR	✔	✔	✔	✔	✔	✔
FCR	✔	✗	✗	✗	✗	✗

OBR

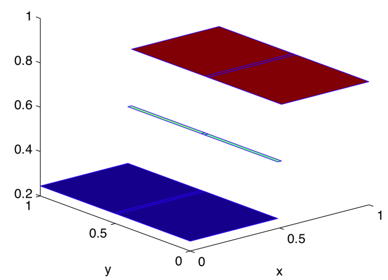

FCR

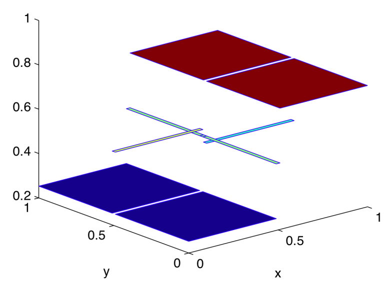

Donor

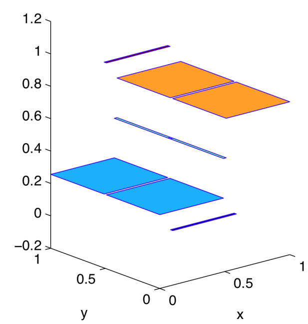

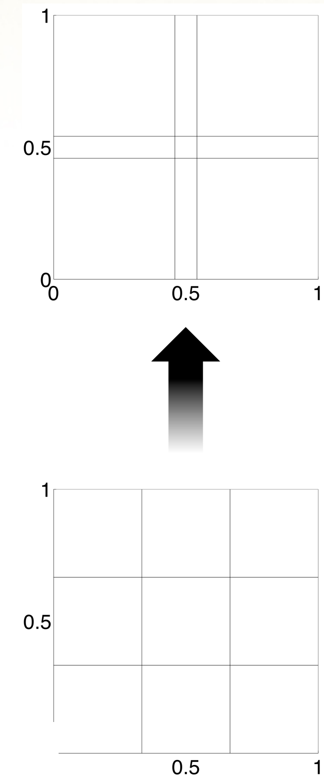

Mesh motion

OBR-FVFT Accuracy: Hourglass Mesh Motion

OBR

Cells	Remaps	L_2 error	L_1 error	L_∞ error	L_2 rate	L_1 rate	L_∞ rate
64	320	1.52E-3	1.23E-3	3.87E-3	—	—	—
256	1280	8.96E-5	7.50E-5	2.44E-4	**2.04**	**2.02**	**1.99**
1024	5120	5.54E-6	4.68E-6	1.54E-5	**2.03**	**2.01**	**1.99**
4096	20480	3.45E-7	2.93E-7	1.39E-6	**2.02**	**2.01**	**1.92**

FCR

Cells	Remaps	L_2 error	L_1 error	L_∞ error	L_2 rate	L_1 rate	L_∞ rate
64	320	7.71e-3	5.96E-3	1.57E-2	—	—	—
256	1280	1.78e-3	1.31E-3	3.81E-3	**1.06**	**1.09**	**1.02**
1024	5120	4.42E-4	3.25E-4	9.51E-4	**1.03**	**1.05**	**1.01**
4096	20480	1.10E-4	8.10E-5	2.38E-4	**1.02**	**1.03**	**1.01**

OBR remains 2nd order (best possible);

FCR accuracy reduced to 1st order

Sandia National Laboratories

Optimization-based monotone transport (OBT)

Dukowicz and Baumgardner (JCP 2000) point out that

incremental remap = transport algorithm.

Incremental remapping such as CSLAM (Lauritzen et al JCP 2010) handles passive tracer transport in climate modeling and simulation.

However, CSLAM and many other existing methods require structured grids, and all rely on **monotone reconstruction methods**, a.k.a. **limiters**.

Optimization-Based Transport (OBT) extends OBR to transport:

- inherits the robustness & accuracy of OBR
- impervious to cell shapes

⇒ **monotone and linearity preserving transport scheme on arbitrary cells!**

Bochev, Ridzal, Young, *Optimization-based modeling with applications to transport. Parts 1-3,* **Springer Lecture Notes in Computer Science**, *LNCS 7116, 2012.*

Incremental remap as transport scheme

Mass is conserved in Lagrangian volumes: $\frac{d}{dt} m_i(t) = \frac{d}{dt} \int_{\kappa_i(t)} \rho(x) dV = 0$

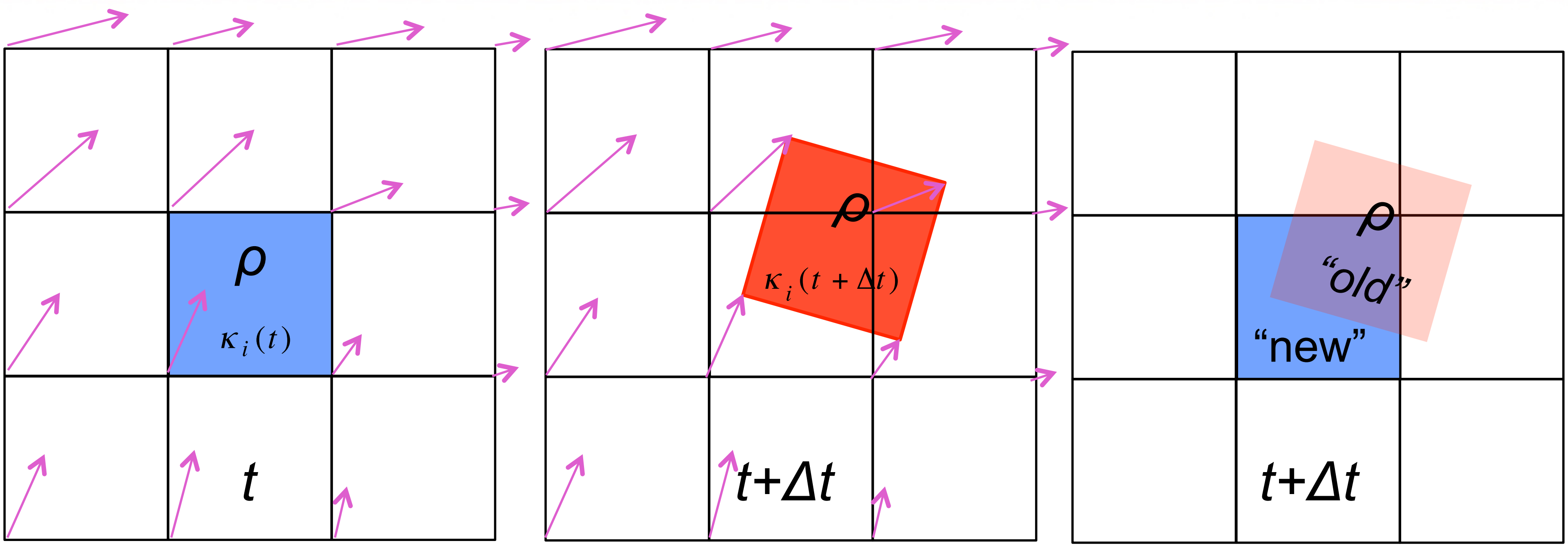

$m_i(t) = \int_{\kappa_i(t)} \rho(x) dV$

$m_i(t+\Delta t) = m_i(t)$

Remap

Optimization-based Remap (OBR) ⇒ OBT algorithm

OBT inherits the robustness of OBR

Zalesak cylinder: rotation

L1 Error	CFL=1	CFL=1.60	CFL=1.62	CFL=2.20	CFL=2.25	CFL=5.21	CFL=5.50
OBT	2.14E-02	2.37E-02	2.38E-02	2.60E-02	2.62E-02	4.02E-02	4.36E-02
FCRT	1.97E-02	2.19E-02	2.21E-02	3.00E-02	**6.00E+06**	**9.45E+38**	**1.83E+40**
VLT	2.14E-02	2.36E-02	8.15E-01	**3.47E+54**	**2.85E+56**	**2.83E+79**	**6.23E+77**

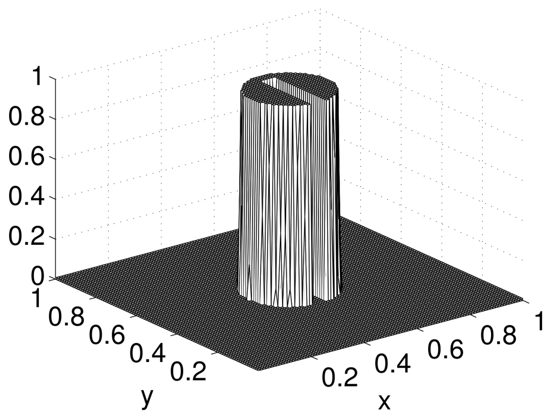

Initial density

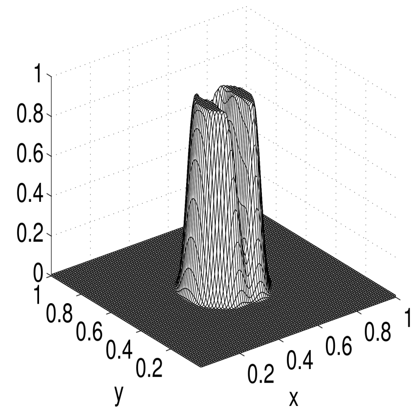

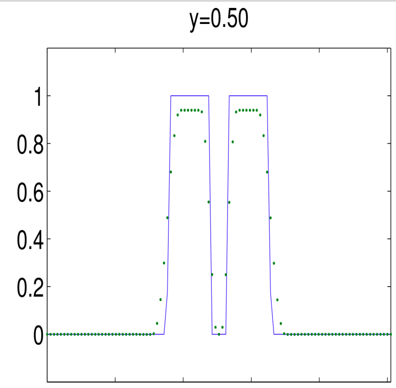

OBR: CFL=1.0

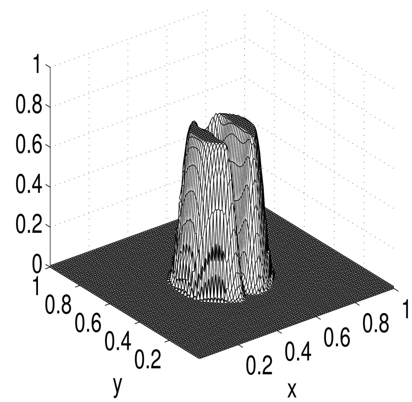

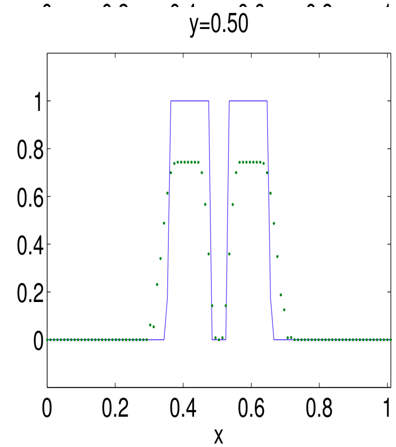

OBR: CFL=4.7

OBT applied to a 2D test example

Rotating flow example (LeVeque, SINUM 33, 1996)

$$u = -(y - 0.5) \qquad v = (x - 0.5)$$

Grid size: *N*x*N*, ***N*=100**

Time steps: $2\pi N$ **628**

CFL < 1

Initial

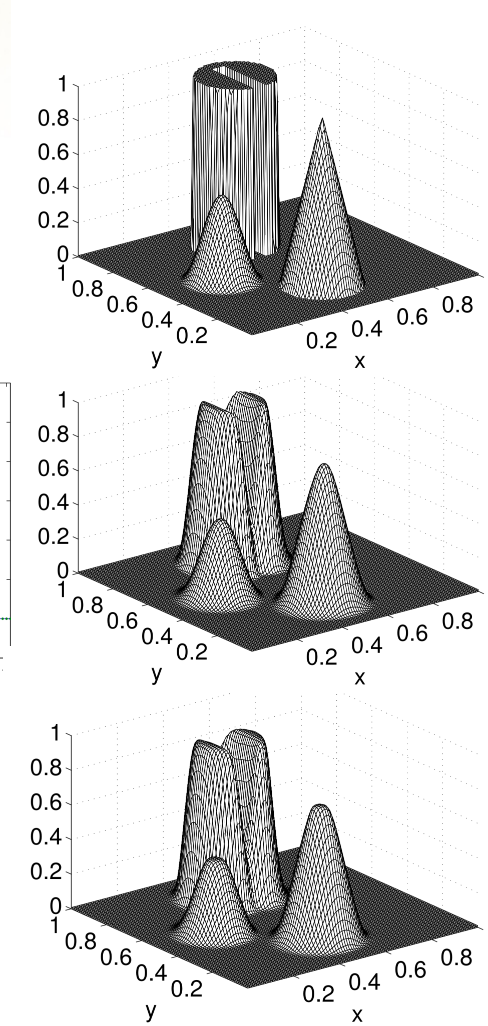

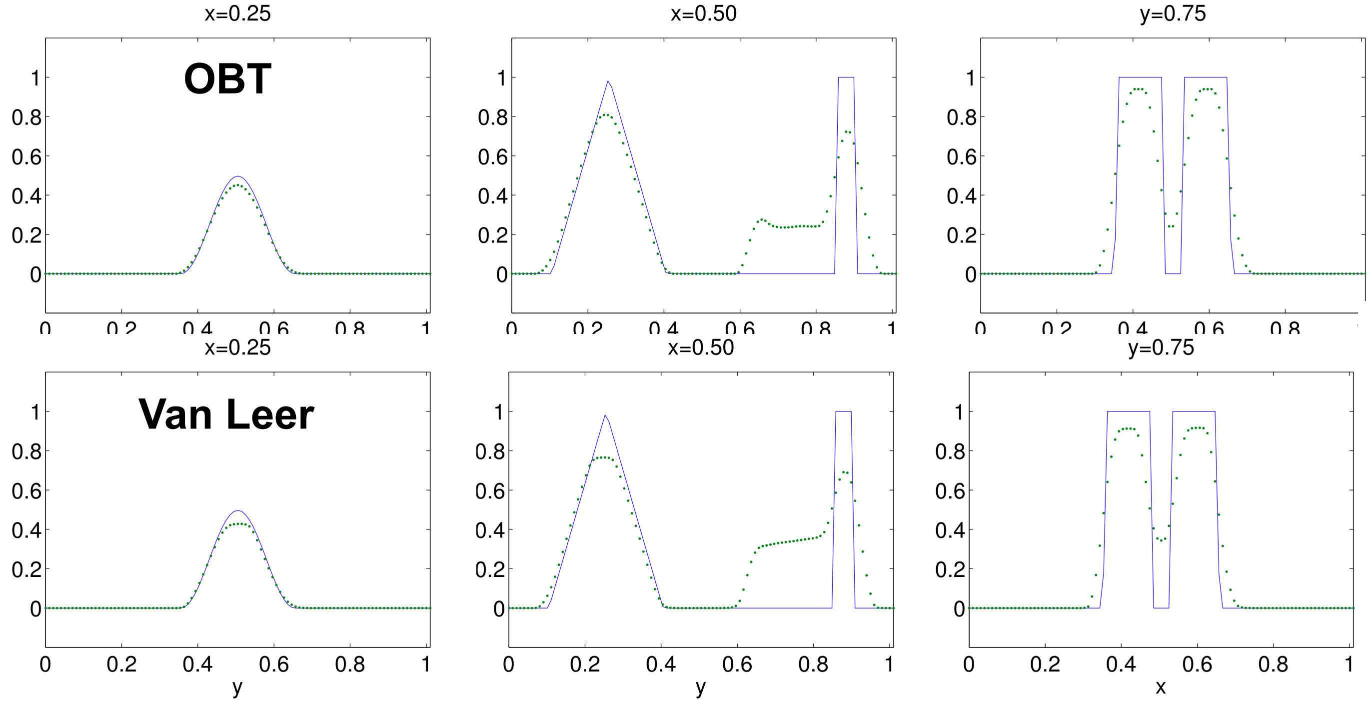

This example combines “**smooth**” and “**sharp**” features!

OBT with adaptive targets

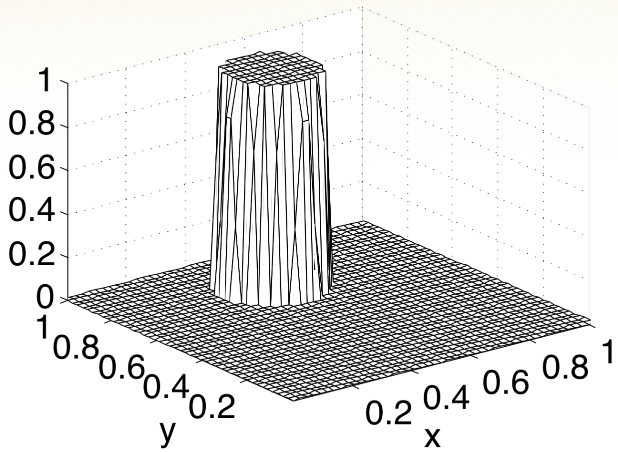

Initial

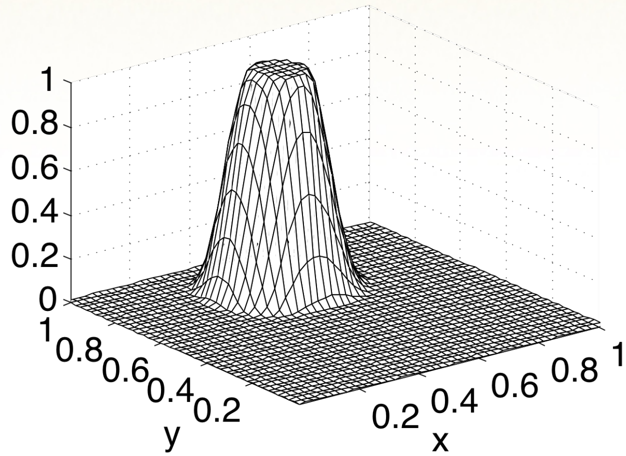

OBT

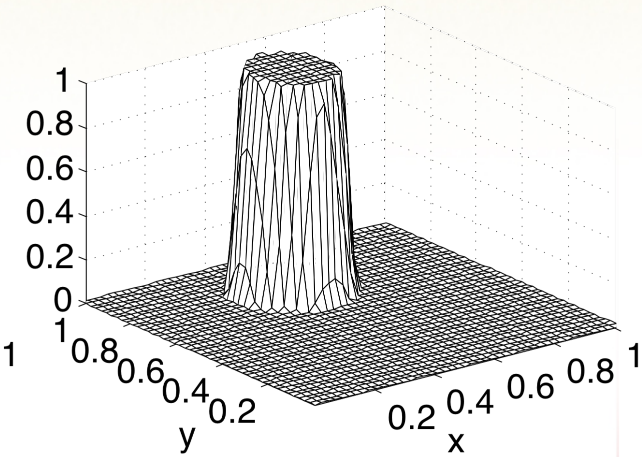

OBT-A

Rotating cylinder

$u = -(y - 0.5) \qquad v = (x - 0.5)$

Grid size: *N*x*N*, ***N*=45**

Time steps: $2\pi N$ **282**

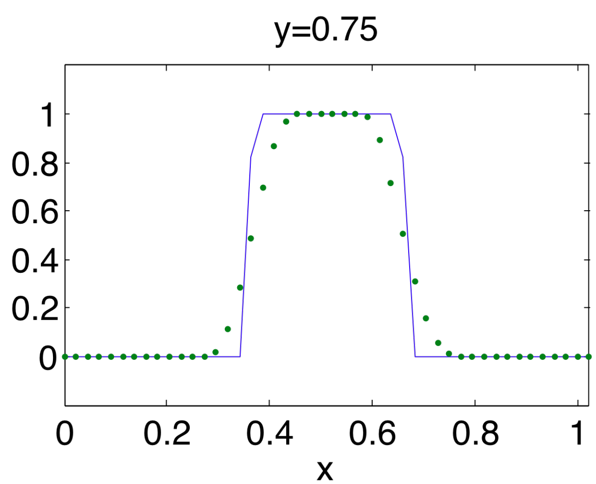

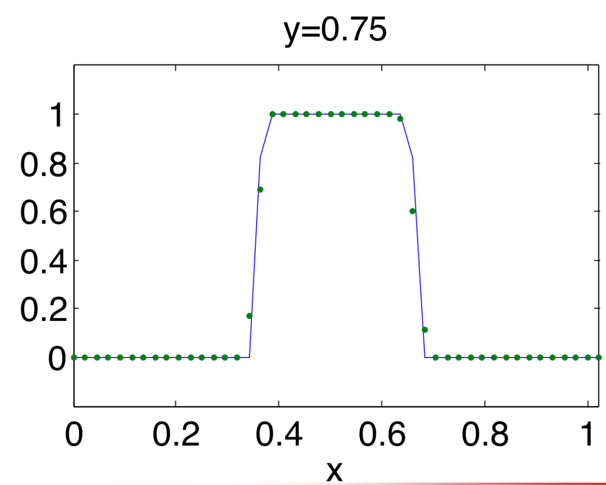

Sandia National Laboratories

OBT with adaptive targets: fine grid

Rotating flow example (LeVeque, SINUM 33, 1996)

$$u = -(y - 0.5) \qquad v = (x - 0.5)$$

Grid size: NxN, **N=100**

Time steps: $2\pi N$ **628**

CFL < 1

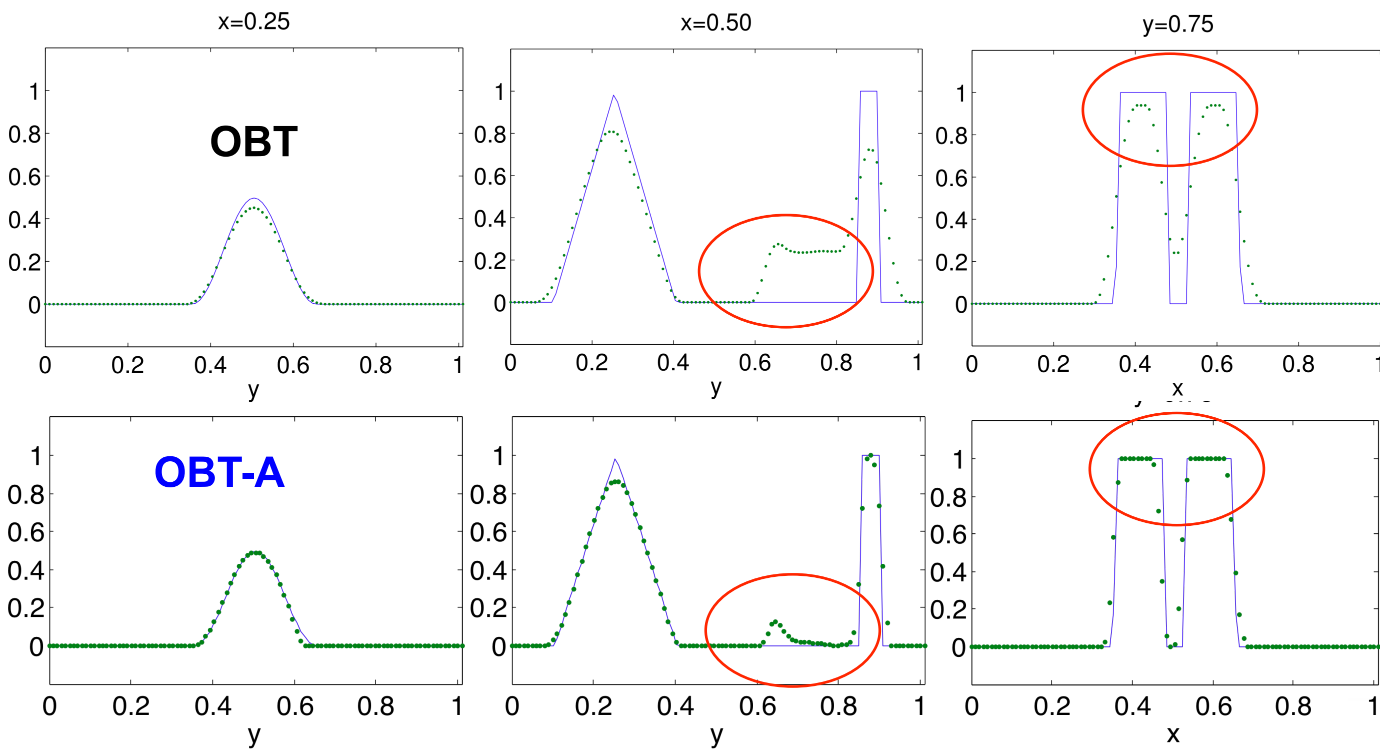

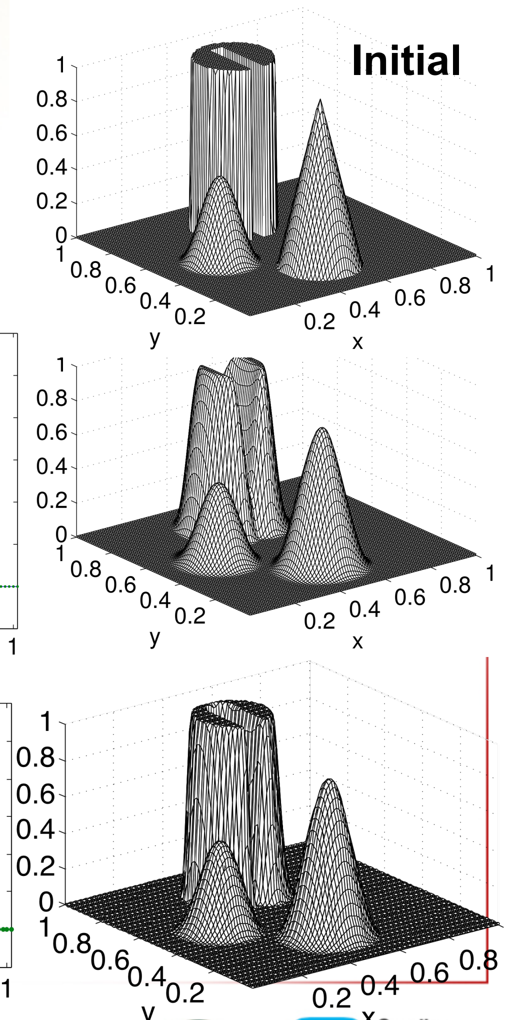

Sandia National Laboratories

OBT with adaptive targets: coarse grid

Rotating flow example (LeVeque, SINUM 33, 1996)

$$u = -(y - 0.5) \qquad v = (x - 0.5)$$

Grid size: *N*x*N*, ***N*=45**

Time steps: 2*πN* **282**

CFL < 1

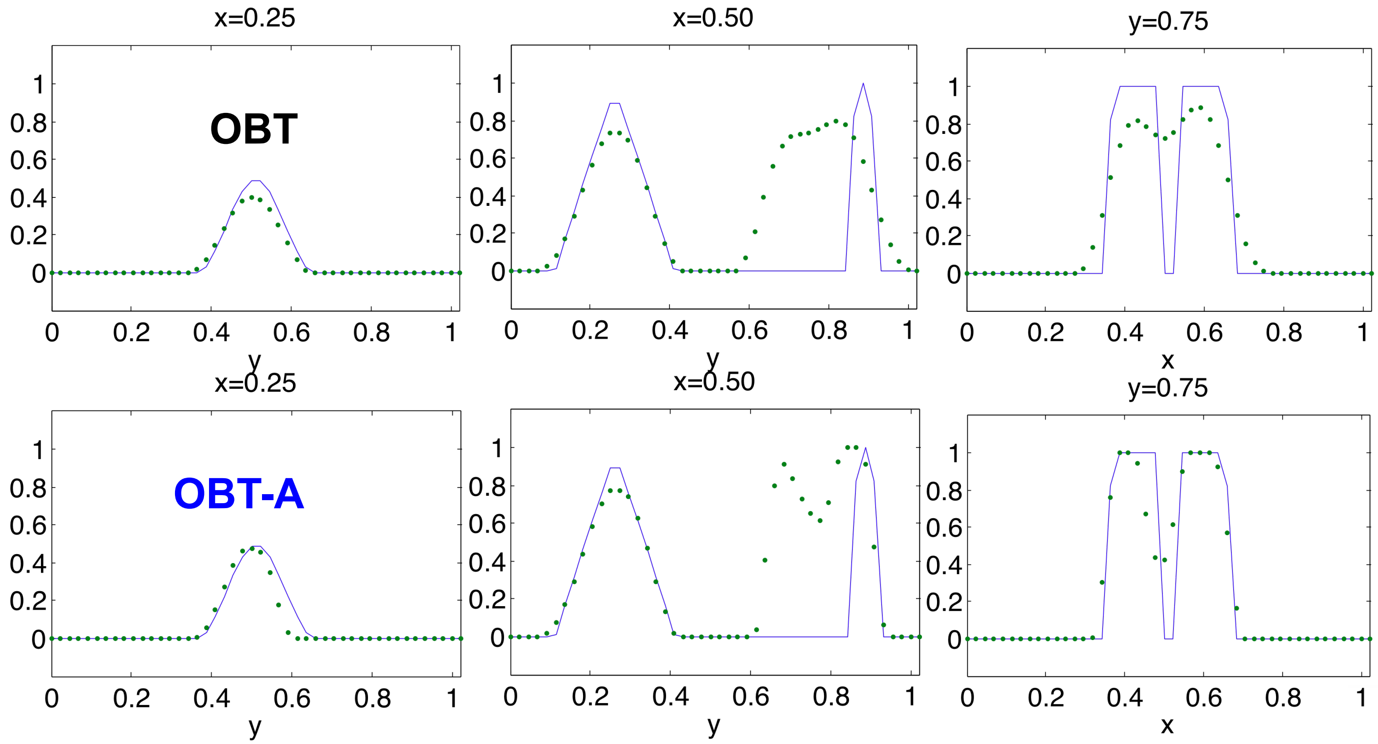

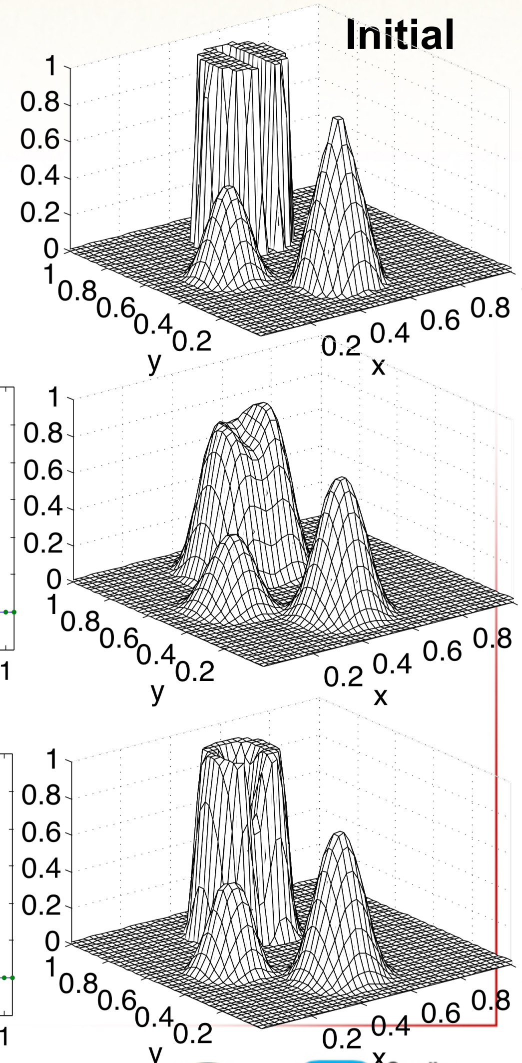

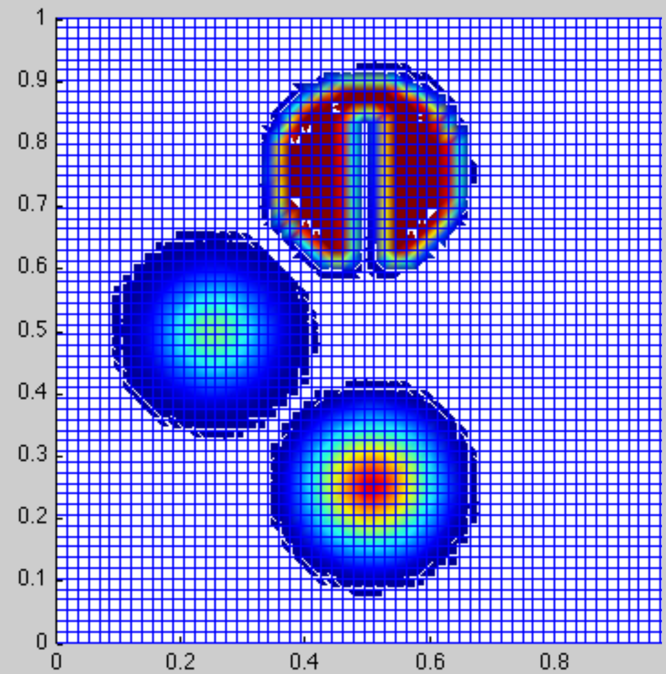

ADAPTIVE OBT

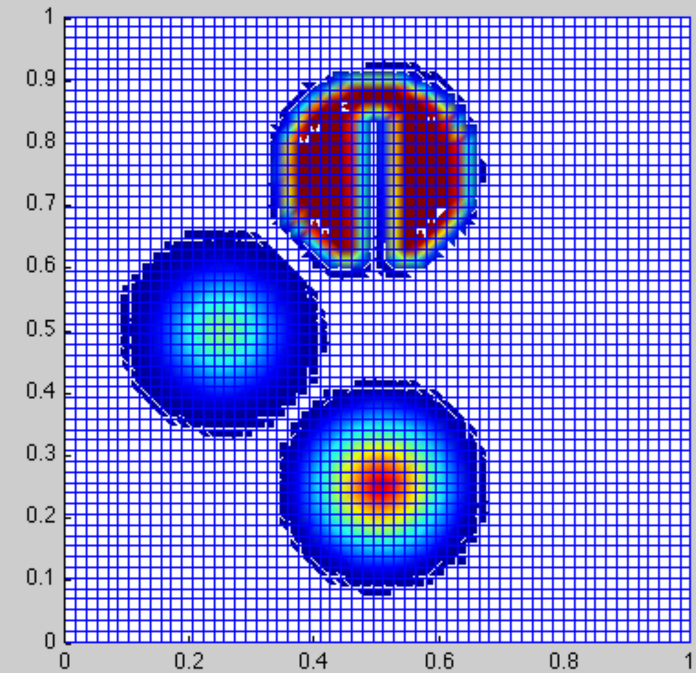

OBT

Cost in remap applications

"Sine"

Cells	Remaps	FCR (sec)	OBR-FVFT	Ratio
64x64	320	4.1	7.3	**1.7**
128x128	640	25.4	49.5	**1.9**
256x256	1280	177.5	390.6	**2.2**
512x512	2560	2049.1	3663.8	**1.8**

"Peak"

Cells	Remaps	FCR (sec)	OBR-FVFT	Ratio
64x64	320	4.9	7.4	**1.6**
128x128	640	28.0	53.9	**1.9**
256x256	1280	194.5	400.8	**2.1**
512x512	2560	2060.1	4410.5	**2.1**

"Shock"

Cells	Remaps	FCR (sec)	OBR-FVFT	Ratio
64x64	320	4.6	9.0	**2.0**
128x128	640	27.4	85.1	**3.1**
256x256	1280	192.5	414.4	**2.2**
512x512	2560	2064.9	3177.1	**1.5**

***Matlab* wall-clock times on a single Intel Xeon X5680 3.33 GHz processor**

Cost in transport applications

"Cone"

Cells	Time steps	FCR (sec)	Van Leer	OBR-FVFT	Ratio
64x64	400	4.59	4.50	44.32	**9.8**
128x128	810	44.64	47.25	757.30	**17.0**
256x256	1,610	387.88	39[illegible]	4,295.71	**11.07**
512x512	3,220	5,715.08	[illegible],8[illegible].66	26,410.87	**4.6**

Reject

"Combo"

Cells	Time steps	FCR (sec)	Van Leer	OBR-FVFT	Ratio
64x64	400	4.51	4.55	34.86	**7.7**
128x128	810	47.60	48.35	737.89	**15.5**
256x256	1,610	390.47	399.15	5545.9	**14.2**
512x512	3,220	5802.05	5804.66	50,940	**8.8**

***Matlab* wall-clock times on a 3.06GHz Intel Core Duo MacBook Pro**

Switch to mass-form of remap

The exact mass on new cell $\tilde{\kappa}_i$ can be expressed in aggregate mass-transfer form:

$$\tilde{m}_i^{EX} = m_i^{EX} + \delta m_i^{EX}; \quad \delta m_i^{EX} = \int_{\tilde{\kappa}_i} \rho(x)dV - \int_{\kappa_i} \rho(x)dV$$

Therefore, the mass on the new cell $\tilde{\kappa}_i$ can be approximated by

$$\tilde{m}_i^h = m_i^h + \delta m_i^h, \quad \text{where} \quad \delta m_i^h = \int_{\tilde{\kappa}_i} \rho_i^h(x)dV - \int_{\kappa_i} \rho_i^h(x)dV \approx \delta m_i^{EX}$$

C1: Mass conservation. Not free anymore: requires a single linear constraint:

$$\sum_{Cell} \delta m_i^h = 0 \quad \Rightarrow \quad \sum_{Cell} \tilde{m}_i^h = M$$

C2: Linearity preservation. Guaranteed if ρ_i^h is exact for linear functions on all κ_i:

$$\delta m_i^T = \int_{\tilde{\kappa}_i} \rho_i^h(x)dV - \int_{\kappa_i} \rho_i^h(x)dV$$ → Target (**high-order**) mass-transfers

C3: Local bounds $\Rightarrow$ $\delta \tilde{m}_i^{min} \le \sum_{cell} \delta m_i^h \le \delta \tilde{m}_i^{max} \quad i = 1,\ldots,N$ → **Box constraints**

Optimization-based remap (OBR): MVMT form

OBR-MVMT = "*singly linearly constrained QP with simple bounds*"

$$\underset{\delta m_i^h}{\text{minimize}} \quad \sum_{Cell} \left(\delta m_i^h - \delta m_i^T\right)^2 \quad \text{subject to}$$

$$\delta \tilde{m}_i^{min} \le \delta m_i^h \le \delta \tilde{m}_i^{max} \qquad i = 1,\ldots,N$$

$$\sum_{Cell} \delta m_i^h = 0$$

⬅ C2

⬅ C3

⬅ C1

Theorem. (Existence of unique optimal solutions)

The OBR-MVMT feasible set is non-empty: for any given density distribution there exists a set of aggregate mass transfers δm_i^h which satisfy the box constraints and sum up to zero

Fast Optimization Algorithm for OBR-MVMT

Key property of singly linearly constrained QP with simple bounds:

$$\underset{\delta m_i^h}{\text{minimize}} \quad \sum_{Cell} \left(\delta m_i^h - \delta m_i^T\right)^2 \quad \text{subject to}$$

$$\delta\tilde{m}_i^{min} \le \delta m_i^h \le \delta\tilde{m}_i^{max}; \; i = 1,\ldots,N \quad \text{and} \quad \sum_{Cell} \delta m_i^h = 0$$

Without the equality constraint the QP is fully separable into N one-dimensional QPs with simple bounds

The Lagrangian

$$L(\delta m, \lambda, \mu_1, \mu_2) = \sum_{Cell} \left(\delta m_i^h - \delta m_i^T\right)^2 - \lambda \sum_{Cell} \delta m_i^h - \sum_{Cell} \mu_{1,i}(\delta m_i^h - \delta\tilde{m}_i^{min}) - \sum_{Cell} \mu_{2,i}(\delta m_i^h - \delta\tilde{m}_i^{max})$$

The Karush-Kuhn-Tucker (KKT) conditions

$$\begin{cases} \delta m_i^h = \delta m_i^T + \lambda + \mu_{1,i} - \mu_{2,i} \\ \delta\tilde{m}_i^{min} \le \delta m_i^h \le \delta\tilde{m}_i^{max} \\ \mu_{1,i} \ge 0, \quad \mu_{2,i} \ge 0 \\ \mu_{1,i}(\delta m_i^h - \delta\tilde{m}_i^{min}) = 0, \\ \mu_{2,i}(\delta m_i^h - \delta\tilde{m}_i^{max}) = 0 \end{cases} \quad \text{and} \quad \sum_{Cell} \delta m_i^h = 0$$

Without the equality constraint the KKT conditions are fully separable and can be solved for any fixed value of λ.

Fast Optimization Algorithm for OBR-MVMT

Step 1: solve for λ fixed

$$\delta m_i^h = \delta m_i^T + \lambda \qquad \mu_{1,i} = 0 \qquad \mu_{2,i} = 0 \qquad \text{if} \quad \delta\tilde{m}_i^{min} \le \delta m_i^T + \lambda \le \delta\tilde{m}_i^{max}$$

$$\delta m_i^h = \delta\tilde{m}_i^{min} \qquad \mu_{2,i} = 0 \qquad \mu_{1,i} = \delta m_i^h - \delta m_i^T - \lambda \qquad \text{if} \quad \delta\tilde{m}_i^{min} \ge \delta m_i^T + \lambda$$

$$\delta m_i^h = \delta\tilde{m}_i^{max} \qquad \mu_{1,i} = 0 \qquad \mu_{2,i} = \delta m_i^T - \delta m_i^h + \lambda \qquad \text{if} \quad \delta m_i^T + \lambda \ge \delta\tilde{m}_i^{max}$$

$$\Rightarrow \quad \delta m_i^h(\lambda) = median(\delta\tilde{m}_i^{min}, \delta m_i^T + \lambda, \delta\tilde{m}_i^{max}); \quad i = 1,\ldots,N$$

Step 2: adjust λ in an outer iteration to satisfy the single equality constraint

Solve $\sum_{Cell} \delta m_i^h(\lambda) = 0$ $\Rightarrow$ **piecewise linear, monotonically increasing function of single scalar variable λ.**

- Can solve to machine precision by a simple secant method
- Globalization is unnecessary because $\lambda_0 = 0$ is an excellent initial guess:

$$\delta m_i^h(\lambda_0) = median(\delta\tilde{m}_i^{min}, \delta m_i^T, \delta\tilde{m}_i^{max}); \quad i = 1,\ldots,N$$

- $\delta m_i^h(\lambda_0)$ solves the QP without the equality constraint, i.e., "almost" a solution
- Locality $\Rightarrow \delta m_i^h(\lambda_0)$ barely violates the mass conservation constraint

Sandia National Laboratories

OBR-MVMT does not compromise robustness & accuracy

Preservation of monotonicity

	C=5	C=6	C=7	C=14	C=15	C=16	C=100
FVFT	✔	✔	✔	✔	✔	✔	✔
MVMT	✔	✔	✔	✔	✔	✔	✔
FCR	✔	✔	✔	✗	✗	✗	✗

Preservation of linearity

	C=3	C=4	C=5	C=15	C=16	C=100
FVFT	✔	✔	✔	✔	✔	✔
MVMT	✔	✔	✔	✔	✔	✔
FCR	✔	✗	✗	✗	✗	✗

Rates of convergence

Sine & repeated repair		***OBR-FVFT***		***OBR-MVMT***	
#Cells	#remaps	L_1 error	L_1 rate	L_1 error	L_1 rate
128x128	640	2.69E-04	-	2.77E-04	-
256x256	1280	6.71E-05	2.01	6.82E-05	2.04
512x512	2560	1.68E-05	2.01	1.69E-05	2.03

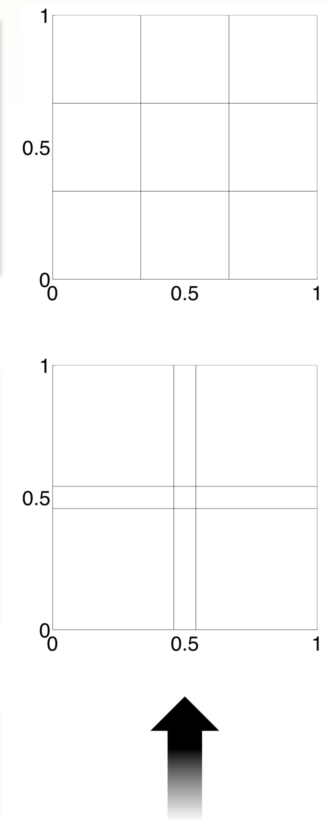

Mesh motion

OBR-MVMT cost: remap applications

“Sine”

Cells	Remaps	FCR (sec)	OBR-FVFT	Ratio	OBR-MVMT	Ratio
64x64	320	4.1	7.3	1.7	4.1	1.0
128x128	640	25.4	49.5	1.9	24.6	1.0
256x256	1280	177.5	390.6	2.2	173.1	1.0
512x512	2560	2049.1	3663.8	1.8	1918.0	0.9

“Peak”

Cells	Remaps	FCR (sec)	OBR-FVFT	Ratio	OBR-MVMT	Ratio
64x64	320	4.9	7.4	1.6	4.9	1.0
128x128	640	28.0	53.9	1.9	28.6	1.0
256x256	1280	194.5	400.8	2.1	192.8	1.0
512x512	2560	2060.1	4410.5	2.1	2096.5	1.0

“Shock”

Cells	Remaps	FCR (sec)	OBR-FVFT	Ratio	OBR-MVMT	Ratio
64x64	320	4.6	9.0	2.0	4.9	1.1
128x128	640	27.4	85.1	3.1	29.1	1.0
256x256	1280	192.5	414.4	2.2	195.6	1.0
512x512	2560	2064.9	3177.1	1.5	2146.7	1.0

***Matlab* wall-clock times on a single Intel Xeon X5680 3.33 GHz processor**

Sandia National Laboratories

OBR-MVMT cost: transport applications

"Cone"

Cells	Time steps	FCR (sec)	Van Leer	OBR-FVFT	Ratio	OBR-MVMT	Ratio
64x64	400	4.59	4.50	44.32	**9.8**	**4.92**	**1.1**
128x128	810	44.64	47.25	757.30	**17.0**	**48.62**	**1.1**
256x256	1,610	387.88	393.64	4,295.71	**11.07**	**403.23**	**1.0**
512x512	3,220	5,715.08	5,804.66	26,410.87	**4.6**	**5655.06**	**0.9**

"Combo"

Cells	Time steps	FCR (sec)	Van Leer	OBR-FVFT	Ratio	OBR-MVMT	Ratio
64x64	400	4.51	4.55	34.86	**7.7**	**4.98**	**1.1**
128x128	810	47.60	48.35	737.89	**15.5**	**48.78**	**1.0**
256x256	1,610	390.47	399.15	5545.9	**14.2**	**405.92**	**1.0**
512x512	3,220	5802.05	5804.66	50,940	**8.8**	**5,655**	**0.9**

***Matlab* wall-clock times on a 3.06GHz Intel Core Duo MacBook Pro**